Simultaneous topology and anisotropy optimization by means of a gradient-based algorithm

Lander Vertonghen, François-Xavier Irisarri, Boris Desmorat, Dimitri Bettebghor

SIMULTANEOUS TOPOLOGY AND ANISOTROPY OPTIMIZATION BY MEANS OF A GRADIENT-BASED ALGORITHM

Lander, Vertonghen[a], François-Xavier, Irisarri[a], Boris, Desmorat[b], Dimitri, Bettebghor[a]

a: DMAS, ONERA, Université Paris Saclay – lander.vertonghen@onera.fr
b: Sorbonne Université, CNRS, UMR 7190, Institut d'Alembert

Abstract:

Solutions to topology optimization problems are strongly influenced by the consideration and simultaneous anisotropy optimization. To broaden anisotropy consideration in topology optimization to other optimization objective and/or constraints, such as strength or buckling, this work introduces a novel way of incorporating 2D orthotropy in a gradient-based optimization routine. The orthotropy is represented by means of the polar formalism, and the optimization strategy uses a combination of the Method of Moving Asymptotes (MMA) and Global Convergent Method of Moving Asymptotes (GCMMA), whichever approximation is better suited to the variable type. As gradient-based optimization are prone to local minima, it is shown that with a proper initialization, the split "MMA" strategy obtains similar compliance values and variable distribution as the alternate directions benchmark algorithm, validating the strategy for further use.

Keywords: topology; optimization; polar parameters

1. Introduction

Topology optimization seeks to define the optimal material distribution of a structure for a defined load case. It is a well-documented problem for compliance minimization with an isotropic material [1], however other properties influence the final solution and topology. This effect can for example be seen in optimizations considering strength and/or buckling constraints [2]. The resolution of such optimization problems with additional constraint is either done with genetic [3] or gradient based [1,2,4] algorithms in literature.

Another influence on the optimized shape is the type and amount of material variables, such as incorporating material anisotropy. General material orthotropy was considered in topology optimizations by Ranaivomiarana *et al.* [5]. Another subset of anisotropy can be mentioned, being the composite laminate space, and having their equivalent stiffness represented and optimized by means of lamination parameters, as performed by Peeters *et al.* [4], with a subsequent fiber path retrieval step.

Ranaivomiarana *et al.* [5] demonstrated that the concurrent consideration of orthotropy in topology optimization resulted in different final topologies, being potential less bulky yet better designs than a sequential optimization of first the topology with an isotropic material, followed by the material orthotropy optimization. However, the optimization method used by Ranaivomiarana *et al.* [5] is based on the alternate directions (AD) method [6] which can only be used for compliance minimization.

In order to incorporate additional constraints in topology optimization whilst considering material anisotropy, the algorithm to solving the optimizations must be switched to a gradient-based method. This is the purpose of the presented work, and is done more specifically with the Methods of Moving Asymptotes (MMA) algorithm [7]. The material anisotropy is still characterized by means of the polar parameters [8], facilitating a comparison of the results of the proposed approach to the ones obtained by Ranaivomiarana *et al.* [5]. Moreover, this still leaves the later possibility to limit the design space to composite layups by means of the geometric bounds on the polar parameters [9].

This remainder of this abstract is setup as follow: Section 1 discusses the background of the topology and anisotropy modelling, the optimization strategy is laid out in Section 2, followed by the presentation and discussion of the results in Section 3 and finally the abstract is concluded in Section 4.

2. Methodology

2.1 Topology representation

The topology variables are the element densities ρ, which are used in the Solid Isotropic Material with Penalization (SIMP) [1] given in Eq. (1) to achieve distinct results. D is the elasticity tensor as used in the definition of an element's stiffness matrix in the finite element method (FEM) analysis, p is the penalization exponent and D_0 the pristine elasticity tensor of an element. Section 1.2 gives the definition of this elasticity tensor D_0 with anisotropy.

$$D = \rho^p D_0 \tag{1}$$

To prevent checkerboard instabilities, a linear filter is used to smoothen the density variables and obtain a length scale control, according to Eq. (2). Ω_i is the set of elements whose centroid distance lays within the filter radius R, and are given a filter weight w_{ij} according to Eq. (3). *x* represents each element's centroid location, and V the element's area.

$$\widetilde{\rho_i} = \frac{\sum_{j\in\Omega_i} w_{ij} V_j \rho_j}{\sum_{j\in\Omega_i} w_{ij} V_j} \tag{2}$$

$$\Omega_i = \{j \mid |x_j - x_i| \leq R\} \text{ and } w_{ij} = R - |x_j - x_i| \tag{3}$$

2.2 Anisotropic representation

The anisotropic behavior of the material is represented by means of the polar formalism [10]. In this communication, the anisotropy is restricted to orthotropy. The components of the pristine elasticity tensor D_0 are obtained by means of the polar parameters [8], expressed in Eq. (4) with normalized anisotropic modules η_0 and η_1. T_0 and T_1 are the isotropic modules, ϕ_1 is the direction of orthotropy. η_0 and η_1 are defined as $\frac{(-1)^K R_0}{T_0}$ and $\frac{R_1}{\sqrt{T_0 T_1}}$ respectively, where R_0 and R_1 are the anisotropic modules and K the orthotropic shape factor.

$$\begin{aligned} D_{1111} &= T_0 + 2T_1 + \eta_0 T_0 \cos 4\phi_1 + 4\eta_1 \sqrt{T_0 T_1} \cos 2\phi_1 \\ D_{1122} &= -T_0 + 2T_1 - \eta_0 T_0 \cos 4\phi_1 \\ D_{1112} &= \eta_0 T_0 \sin 4\phi_1 + 2\eta_1 \sqrt{T_0 T_1} \sin 2\phi_1 \end{aligned} \tag{4}$$

$$D_{2222} = T_0 + 2T_1 + \eta_0 T_0 \cos 4\phi_1 - 4\eta_1\sqrt{T_0 T_1}\cos 2\phi_1$$

$$D_{2212} = -\eta_0 T_0 \cos 4\phi_1 + 4\eta_1\sqrt{T_0 T_1}\sin 2\phi_1$$

$$D_{1212} = T_0 - \eta_0 T_0 \cos 4\phi_1$$

2.3 Thermodynamic bounds

To keep the elasticity tensor D_0 theoretically valid, meaning it remains positive definite, the thermodynamic bounds must be enforced on the anisotropic modules and orthotropic shape factor [8]. These bounds are expressed with the normalized anisotropic modules in Eq. (5), where the strict inequality has been relaxed by introducing $(1-\varepsilon)$. This relaxation is necessary, as the constraints in MMA are simple inequalities. The value of ε is taken as 0.05 in this communication.

$$\eta_0 \geq (1-\varepsilon)\left(2\left(\frac{\eta_1}{(1-\varepsilon)}\right)^2 - 1\right)$$

$$-(1-\varepsilon) \leq \eta_0 \leq (1-\varepsilon) \tag{5}$$

$$-(1-\varepsilon) \leq \eta_1 \leq (1-\varepsilon)$$

However, as the thermodynamic constraint must be considered for each separate element with its own variables, the number of optimization constraints quickly rises and becomes troublesome and slow to handle by the optimization algorithm. Therefore, the thermodynamic constraint is implicitly incorporated as a variable change in a similar way as suggested by Izzi *et al.* [11]. The variable change specific to Eq. (5) is given in Eq. (6), and means the optimization constraint now becomes a simple interval on these new variables.

$$\alpha = \frac{\eta_1 + (1-\varepsilon)}{2(1-\varepsilon)} \;;\; \beta = \frac{\eta_0 - (1-\varepsilon)}{2(1-\varepsilon)\left[\left(\frac{\eta_1}{(1-\varepsilon)}\right)^2 - 1\right]}$$

$$0 \leq \alpha \leq 1 \;;\; 0 \leq \beta \leq 1 \tag{6}$$

2.4 Optimization problem

The optimization problem treated is the minimization of the compliance (C), being the work of the external loads, and defined as the deformation energy ($U^T K U$). U is the displacement vector, obtained from the resolution of $KU = F$, where is K the global stiffness matrix and F the force vector. The optimization problem is stated in Eq. (7), and subjected to a volume V constraint to be lowered than a prescribed volume V_0.

$$\min_{\rho,\phi_1,\eta_0,\eta_1} \quad U^T K U$$

$$s.t.\ V \leq V_0$$

$$0 \leq \alpha \leq 1 \tag{7}$$

$$0 \leq \beta \leq 1$$

$$0.001 \leq \rho \leq 1 \quad ; \quad -\frac{\pi}{2} \leq \phi_1 \leq \frac{\pi}{2}$$

3. Optimization strategy

The MMA optimization algorithm class [7] is used to solve this optimization problem. MMA is an iterative method of solving a non-linear problem by solving a succession of approximate convex problems. These approximated convex problems are constructed based on the gradient information. As the response surface of the problem differs with respect to the nature of the variable, Bruyneel *et al.* [12] therefore suggested using different approximations for different variables [12], to influence on the convergence properties of the optimization. This inspired the following split "MMA" optimization strategy, where each variable type is optimized separately based on what better suits it characteristics.

The density variables are optimized with the standard MMA and its monotonous approximation, shown to behave well in literature [1,2]. Equally, the anisotropic modules and its change of variables are updated with a separate call of MMA and its monotonous approximation, giving good convergence. Having this separate MMA call allows to use a different optimization settings to guide the optimization of the anisotropic components. Finally, the orientations are optimized with the convex approximation of GCMMA, to help mitigate the influence of the periodicity of the variable, and again with its individual settings. An overview of the optimization strategy is given in Fig. (1).

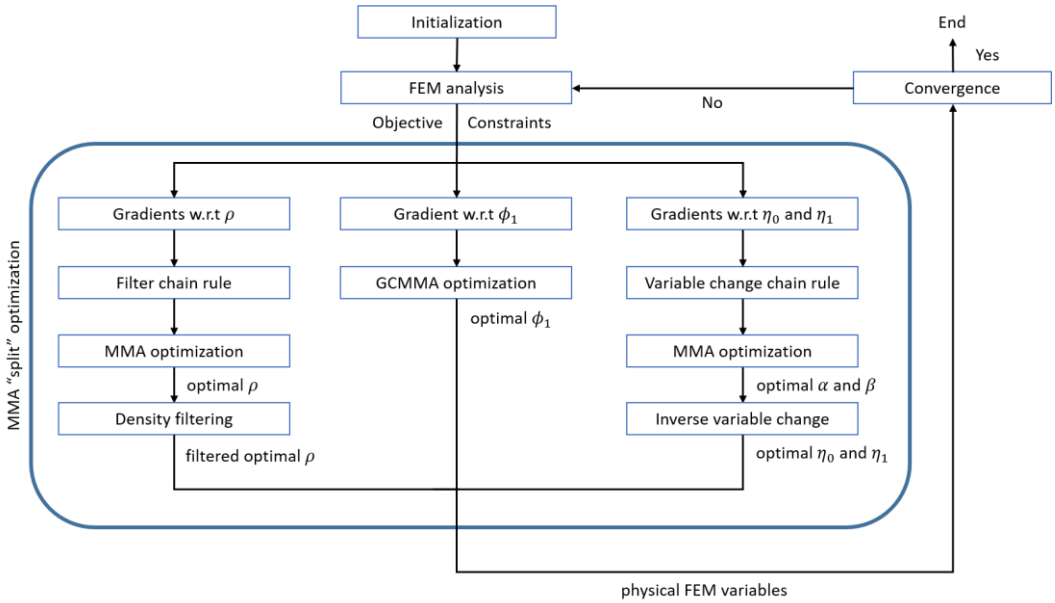

Figure 1. Optimization strategy.

3.1 Sensitivities

As a gradient optimizer is used, the sensitivities of the compliance and volume must be calculated with respect to each variable. The sensitivity with respect to the density is straightforward [1], given in Eq. (8) and Eq. (9), where k_i and u_i are the respective element's stiffness matrix and nodal displacement. V_i is an element's volume.

$$\frac{\partial C}{\partial \tilde{\rho}_i} = -p\tilde{\rho}_i^{p-1} u_i^T k_i u_i \tag{8}$$

$$\frac{\partial V}{\partial \tilde{\rho}_i} = V_i \tag{9}$$

Furthermore, to take the effect of the filter on the optimization variables into account, the chain rule must be applied according to Eq. (10), for any function *f*.

$$\frac{\partial f}{\partial \rho_i} = \sum_{e\in\Omega_i} \frac{\partial f}{\partial \tilde{\rho}_e}\frac{\partial \tilde{\rho}_e}{\partial \rho_i} \text{ , with } \frac{\partial \tilde{\rho}_e}{\partial \rho_i} = \frac{w_{ei}V_i}{\sum_{j\in\Omega_e} w_{ej}V_j} \tag{10}$$

Analogously to the gradient with respect to the density, and using the self-adjoint property of the compliance problem [1], the gradient with respect to the anisotropic components can be obtained as shown in Eq. (11) and Eq. (12) for the direction of orthotropy ϕ_1, and similarly for η_0 and η_1. The sensitivity of the elasticity tensor is obtained from the analytical derivation of Eq. (4), where B is the strain displacement matrix of the element used to setup the FEM analysis.

$$\frac{\partial C}{\partial \phi_i} = -\ u_i^T \frac{\partial k_i}{\partial \phi_i} u_i \tag{11}$$

$$\frac{\partial k_i}{\partial \phi_i} = -\rho_i^p \iint_\Omega B^T \frac{\partial D_{0i}}{\partial \phi_i} B d\Omega \tag{12}$$

Finally, to obtain the gradient with respect to the change of variable to incorporate the thermodynamic bounds, the chain rule as given in Eq. (13) must be applied.

$$\frac{\partial C}{\partial \alpha} = \frac{\partial C}{\partial \eta_0}\frac{\partial \eta_0}{\partial \alpha} + \frac{\partial C}{\partial \eta_1}\frac{\partial \eta_1}{\partial \alpha} \quad ; \quad \frac{\partial C}{\partial \beta} = \frac{\partial C}{\partial \eta_0}\frac{\partial \eta_0}{\partial \beta} + \frac{\partial C}{\partial \eta_1}\frac{\partial \eta_1}{\partial \beta} \tag{13}$$

4. Results and discussion

The suggested methodology and optimization strategy by means of a gradient-based algorithm is compared against reproduced results with the optimization strategy of Ranaivomiarana *et al.* [5], itself based on the alternate directions algorithm [6]. The treated optimization problem consists of a cantilever beam of aspect ratio 2:1, clamped at the left side, and loaded in the middle of the right side. The continuation on the SIMP exponent is p = 3 then p = 5, both exponents used for 100 iteration each for either algorithm.

Furthermore, the same filter radius is used with both algorithms. However, the AD algorithm in [5] is programmed with an energy filter [13], which filters the deformation energy instead of only the densities. The most notable difference from this comes as the energy filter with a given filter radius will result in a topology with little intermediate densities. On the contrary, the density filter with the same active filter radius will have intermediate densities due to the averaging and blurring effect on the boundary of the topology. These intermediate densities penalize the objective interpretation. Therefore, the density filter is removed for the last 25 iterations, to obtain distinct results. This removal results in similar intermediate density levels between both algorithms, measured by the measure of non-discreteness (M_{nd}) [14], and allows the comparison of the optimization objective value.

Gradient-based optimizations are prone to getting trapped in local minima. The optimization solutions are sensitive to the initialization of the variables, the settings of the (GC)MMA optimization algorithm, and continuation strategy on the SIMP exponent. Here, the split “MMA” optimization is initialized with the variable distributions obtained after five iterations with the energy filter and AD algorithm, given in Fig. (2). It can be seen that these variable distributions are still general, however, as discussed later, allow converging to a similar solution as the AD algorithm.

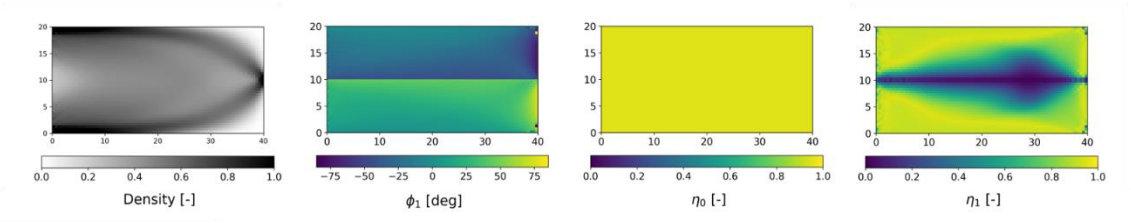

Figure 2. Initialization of the variables, obtained from five iterations with the AD algorithm [5], for the gradient-based optimization.

The results of both optimizations after the final iteration are given in Fig. (3). Similar topology and anisotropy variable distributions are obtained in both cases. Some chequerboard-like phenomenon is visible for η_1 with the gradient-based optimization. This difference could be filter related, where the energy filter in the AD optimization uses the deformation energy of neighboring elements into account, which in itself filters the orientation and anisotropic components. The filter used for the gradient-based optimization is only acting on the densities. Furthermore, comparing the compliance of both optimization reveals close values, with similar levels of M_{nd}: 13.8 mJ with 5.1% of M_{nd} for the AD optimization and 14.0 mJ with 2.9% M_{nd} for the suggested MMA gradient-based strategy.

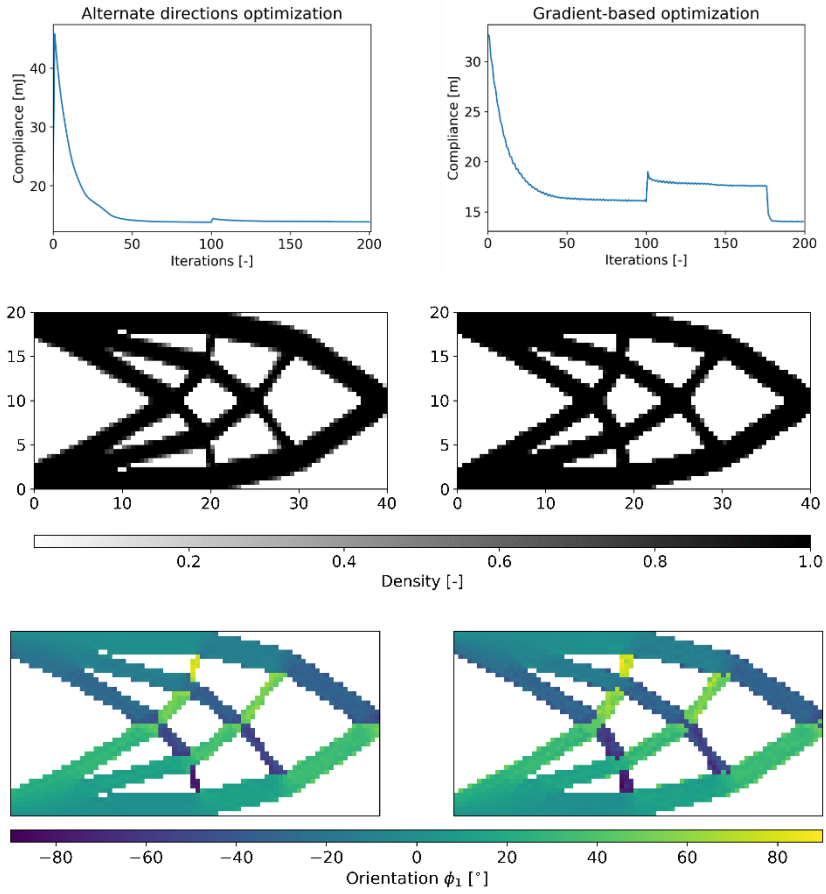

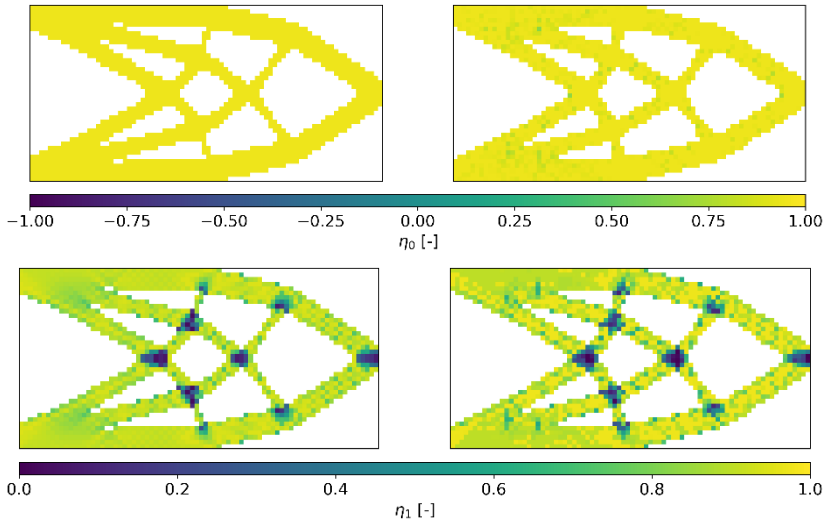

Figure 3. Final variable distribution, on the left for the AD algorithm [5] with energy filter (C = 13.8 mJ, M_{nd} = 5.1%), on the right with the current strategy with density filter (C = 14.0 mJ, M_{nd} = 2.9%). The orientations and anisotropic modules are shown for densities ≥ 0.8.

Analyzing the results more in details, it is particularly interesting to note that the gradient optimization manages to find a theoretical result directly exploited in the case of the AD algorithm, namely that the optimal orientations ϕ_1 are aligned with the maximum of the absolute value of the principal stresses. This observation and the good agreement between variable distributions and objective value allows to validate that the suggested gradient-based strategy is well suited to incorporating anisotropy in topology optimization, and converges to a similar solution to that of a simultaneous optimization with the AD algorithm.

5. Conclusion

The purpose of this paper is to describe a gradient-based optimization strategy capable of considering material anisotropy in topology optimization. The anisotropy is restricted to 2D orthotropy and characterized by means of the polar parameters. The anisotropic modules are bound by the thermodynamic bound, which applies to each separate element. To reduce the computational cost of considering the many thermodynamic constraints during the optimization, these bounds were therefore replaced as a variable change. This variable change results in an implicit optimization interval, furthermore ensuring the thermodynamic condition is always satisfied. Moreover, the optimization strategy relies on the adequate selection of the approximation type of the Method of Moving Asymptotes (MMA), depending on the nature of the variables. This results in the introduction of a “split” MMA strategy, where density and normalized anisotropic modules are optimized separately with each the standard MMA, while the orientations are optimized with GCMMA. Finally, as gradient-based optimization are prone to local minima, a specific initialization to the optimization problem is used to guide the “split” MMA optimization towards a similar topology and variable distribution as the alternate directions benchmark optimization. Furthermore, removing the density filter during the last few iterations reduces the amount of intermediate densities and boundary blurring, to obtain distinct topologies, whose compliance value can be compared to the alternate directions solution of Ranaivomiarana *et al.* [5]. The comparison of variable distribution and compliance between the benchmark and suggested strategy are in agreement. This successful comparison

validates the suggested split "MMA" strategy to consider anisotropy in topology optimization. Hence, this strategy allows for later incorporation of more versatile optimization constraints in topology optimization, such as buckling or strength.

Acknowledgements

The authors are thankful to Airbus Atlantic for funding this research project, and specifically Attilio Chiappini for his help and the interactions with him on the subject.

6. References

1. Bendsøe MP, Sigmund O. Topology Optimization. Berlin, Heidelberg: Springer Berlin Heidelberg; 2004.
2. Gao X, Li Y, Ma H, Chen G. Improving the overall performance of continuum structures: A topology optimization model considering stiffness, strength and stability. Computer Methods in Applied Mechanics and Engineering. 2020; 359:112660.
3. Montemurro M, Pagani A, Fiordilino GA, Pailhès J, Carrera E. A general multi-scale two-level optimisation strategy for designing composite stiffened panels. Composite Structures. 2018; 201:968-79.
4. Peeters D, van Baalen D, Abdallah M. Combining topology and lamination parameter optimisation. Structural and Multidisciplinary Optimization. 2015; 52(1):105-20.
5. Ranaivomiarana N. Simultaneous optimization of topology and material anisotropy for aeronautic structures [Thesis]. Sorbonne Université; 2019.
6. Allaire G, Belhachmi Z, Jouve F. The homogenization method for topology and shape optimization. Single and multiple loads case. Revue européenne de Mécanique Numérique. 2012 May;5(5).
7. Svanberg K. The method of moving asymptotes—a new method for structural optimization. International Journal for Numerical Methods in Engineering. 1987; 24(2):359-73.
8. Vannucci P. Plane Anisotropy by the Polar Method. Meccanica. 2005 Dec;40(4):437-54.
9. Vannucci P. A Note on the Elastic and Geometric Bounds for Composite Laminates. Journal of Elasticity. 2013; 112(2):199-215.
10. Verchery G. Les invariants des tenseurs d'ordre 4 du type de l'élasticité. Mechanical Behavior of Anisotropic Solids/Comportment Méchanique des Solides Anisotropes. 1982; 93-104.
11. Izzi MI, Catapano A, Montemurro M. Strength and mass optimisation of variable-stiffness composites in the polar parameters space. Structural and Multidisciplinary Optimization. 2021; 64(4):2045-73.
12. Bruyneel M, Duysinx P, Fleury C. A family of MMA approximations for structural optimization. Structural and Multidisciplinary Optimization. 2002; 24(4):263-76.
13. Desmorat B. Structural rigidity optimization with frictionless unilateral contact. International Journal of Solids and Structures. 2007; 44(3):1132-44.
14. Sigmund O. Morphology-based black and white filters for topology optimization. Structural and Multidisciplinary Optimization. 2007; 33(4):401-24.

